Poly(*N*-vinylformamide) Nanogels Capable of pH-Sensitive Protein Release

Lianjun Shi,[‡] Supang Khondee,[‡] Thomas H. Linz,[‡,§] and Cory Berkland*[,†,‡]

Departments of Pharmaceutical Chemistry, Chemical and Petroleum Engineering, and Chemistry, The University of Kansas, Lawrence, Kansas 66047

Received April 11, 2008; Revised Manuscript Received July 4, 2008

ABSTRACT: Hydrogel particles have an historic presence in the field of drug formulation and delivery. Applications of particulate forms of gel materials continue to expand as a result of enhanced control over physicochemical properties including particle size, degradability, and environmental responsiveness. Here, acid-labile poly(*N*-vinylformamide) (PNVF) nanogels ~100 nm in diameter were synthesized via inverse emulsion polymerization of *N*-vinylformamide in the presence of a ketal-containing cross-linker. The dissolution half-life of nanogels proved to be dramatically faster at low pH. Nanogels with a monomer:cross-linker ratio of seven demonstrated a 90 min half-life at pH 5.8 compared to ~57 h at pH 7.4. Approximately 95% of lysozyme encapsulated in nanogels released over 200 min at pH 5.8 compared to only ~15% released at pH 7.4. The encapsulation efficiency was moderate with optimal conditions leading to ~60% encapsulation efficiency. In addition, released lysozyme retained about 50% of the original activity. Large differentials in PNVF nanogel dissolution time and protein release in response to slight changes in pH may ultimately provide a mechanism to selectively deliver macromolecular therapeutics to acidic tissues or intracellular vesicles.

Introduction

Hydrogels composed of cross-linked hydrophilic homopolymers or copolymers have been utilized for a multitude of pharmaceutical formulations.[1] As a result of the high water content and excellent biocompatibility of many of these materials, a variety of hydrogels have been developed for delivering active ingredients in the context of tissue engineering[2,3] and controlled release drug delivery.[4] Specifically, controlled release hydrogel materials have been developed as topical,[5] injectable,[6] and oral dosage forms,[7] among others. The hydrophilic nature of hydrogels makes them especially attractive for encapsulating proteins or DNA as compared to hydrophobic matrices, which can adsorb and denature these biologicals.[8] Researchers continue to expand the utility of hydrogels through efforts to control polymer degradability and sensitivity to external stimuli. Translating these benefits to a nanoparticulate form of the hydrogel may also facilitate novel therapeutic applications of hydrogels as injectable colloids capable of selectively delivering drugs intracellularly.

Sustained delivery of active proteins has been achieved from a variety of hydrogel systems. Proteins including interleukins, growth factors, and antibodies have been successfully entrapped and released from hydrogel materials.[9−11] Synthetic strategies to include molecules that bind proteins (e.g., heparin-binding growth factors) have also been utilized to improve protein stability and control release from hydrogel matrices.[12] Recombinant protein technology aims to further augment the utility of hydrogels by allowing the synthesis of gel-forming proteins that possess well-defined physicochemical properties.[13−15]

Cross-linking strategies have also evolved to provide a handle for imparting degradability to hydrogel systems and offer improved flexibility in controlling release. Traditional acrylamide polymerization methods coupled with unique cross-linking strategies have been utilized to produce delivery systems that are biocompatible and capable of maintaining protein structure and function.[16] Photo-cross-linking techniques have also been developed to minimize or eliminate solvents and provide the possibility of in situ gelation.[17] In addition, clever hydrogel systems have been developed that self-assemble in solution through molecular interactions similar to the historic poly-*N*-isopropylacrylamide systems. For example, Hennink and others developed dextran−lactic acid conjugates that produced gels through stereocomplex formation of enantiomeric lactic acid side chains.[18] The resulting hydrogel was completely biodegradable, biocompatible, and capable of controlled release of proteins.[19]

Inverse emulsion polymerization offers an efficient method to translate some of these controlled release approaches to spherical gel particles of micrometer or nanometer size. In the past decade, this method has been exploited to encapsulate proteins and nucleic acids within polyacrylamide gel particles.[20] Emerging applications aim to use micro- or nanogels as diagnostic agents, vaccines, enzymatic reactors, and a mode to facilitate intracellular drug delivery.[21,22] Nanogels less than a few hundred nanometers in diameter may ultimately augment some of these applications since nanoparticles of this size offer the ability to penetrate blood capillaries and tissues and can be taken up by cells.[23] As a result, nanogels may serve as desirable carriers to deliver biological agents with intracellular activity while offering the possibility of extending the circulation half-life of encapsulated biologicals.

In this report, inverse microemulsion polymerization was employed to produce acid-labile poly(*N*-vinylformamide) (PNVF) nanogels (Figure 1A). The monomer *N*-vinylformamide (NVF) was selected since it is water-soluble and possesses much lower toxicity than acrylamide.[24] An acid-labile cross-linker, 2-bis[2,2′-di(*N*-vinylformamido)ethoxy]propane (BDEP) was designed and synthesized to possess two polymerizable NVF moieties mirroring a central ketal.[25,26] In an effort to improve protein stability during nanogel fabrication, the free radical copolymerization of NVF and BDEP was initiated at 37 °C by 2,2′-azobis(2,4-dimethylpentanitrile) (VAZO-52), a low-temperature free-radical initiator. The resulting nanogels dissolved nearly 40-fold more quickly at pH 5.8 than at pH 7.4 and released lysozyme significantly faster at lower pH. The small size and pH-sensitive

* To whom correspondence should be addressed: Ph (785) 864-1455; Fax (785) 864-1454; e-mail berkland@ku.edu.
† Department of Pharmaceutical Chemistry.
‡ Department of Chemical and Petroleum Engineering.
§ Department of Chemistry.

10.1021/ma800812z CCC: $40.75
Published on Web 08/09/2008

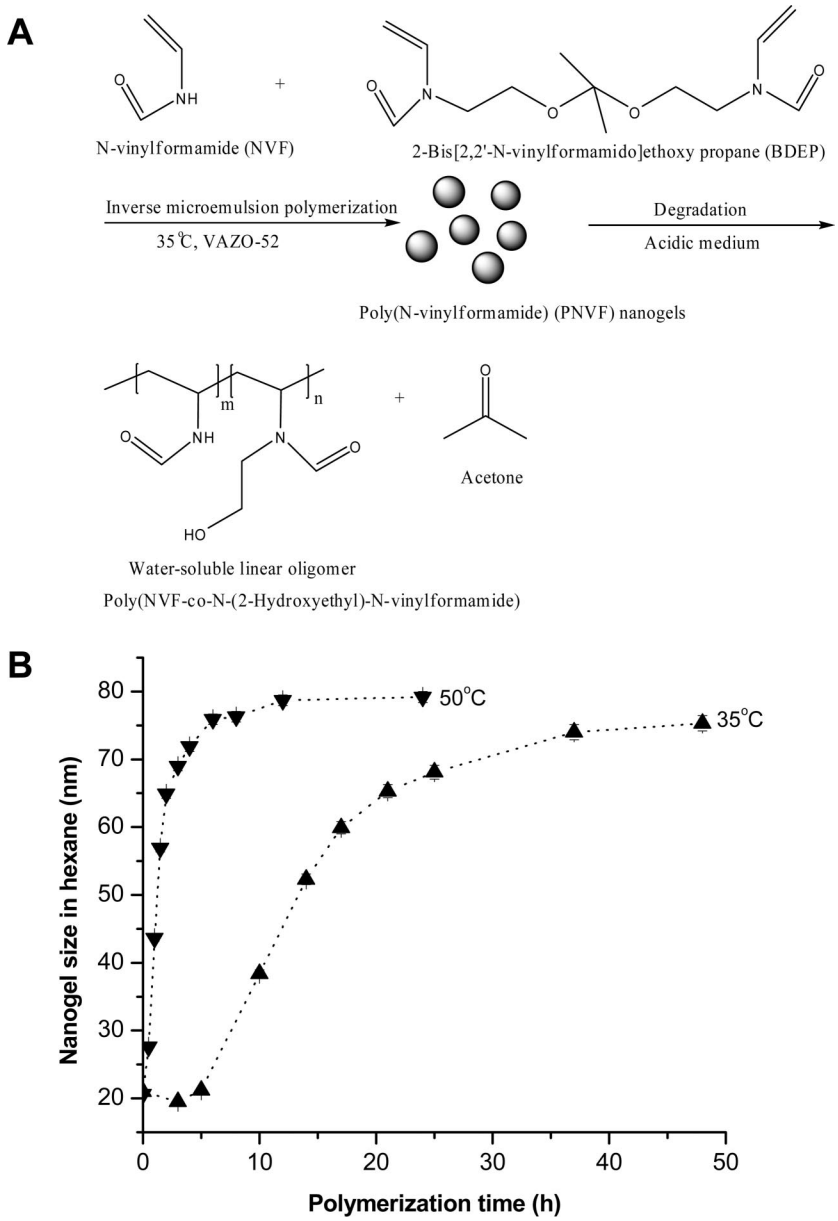

Figure 1. (A) Process for the preparation of acid labile PNVF nanogels. (B) Relationship between acid-labile PNVF nanogel size and polymerization time at 35 and 50 °C was determined using dynamic light scattering. The lower polymerization temperature, desired for protein entrapment, required longer time to achieve similar particle size and process yield.

release of proteins suggest that PNVF nanogels may offer selective protein delivery to acidic tissues or intracellular organelles.

Materials and Methods

Materials. *N*-Vinylformamide (NVF; Aldrich) was distilled under vacuum and stored at −18 °C. 2,2′-Azobis(2,4-dimethylpentanitrile (Vazo-52, purchased from DuPont), a low-temperature free-radical initiator, was employed to initiate polymerization of *N*-vinylformamide. Water used in this research was obtained from a Barnstead EasyPure water purifier. 2-Bis[2,2′-di(*N*-vinylformamido)ethoxy]propane (BDEP) was synthesized according to the procedure previously reported.[25,26] FITC-lysozyme was prepared according to standard protocols as have been reported previously.[27] All other materials were used as received.

Inverse Microemulsion Polymerization of Acid-Labile PNVF Nanogels. Acid-labile PNVF nanogels were fabricated by inverse microemulsion copolymerization of NVF with BDEP. As an exemplary description, microemulsion stock solutions were prepared by mixing 100 mL of hexane stock solution, which contained Tween-80 (3.55 g), Span-80 (4.10 g), and VAZO-52 (30 mg), with an aqueous stock solution, which contained NVF (350 mg), VAZO-52 (16 mg), BDEP (50 mg), and water (200 mg) in a 150 mL bottle followed by homogenization until an optically transparent solution was obtained. Afterward, the microemulsion was transferred into a 150 mL jacketed three-neck flask equipped with a stir bar, which was connected to an Isotemp recirculating water bath. The reactor was sealed with rubber stoppers, and the contents were flushed with nitrogen for 15 min to remove oxygen while stirring at room temperature. Polymerization was carried out at 50 °C for 24 h or 35 °C for 48 h. During the polymerization reaction, the fluid becomes increasingly turbid, which is indicative of nanogel formation. Other polymerization conditions, such as different percentages of cross-linker per mass of monomer, are denoted in the text.

Encapsulation of Lysozyme in Acid-Labile PNVF Nanogels. Encapsulation of lysozyme was carried out via inverse microemulsion polymerization following the same procedure as described above except that the inverse microemulsion was formed

with an aqueous stock solution containing 10 mg of lysozyme. The polymerization conditions are reported in the tables.

Purification of PNVF Nanogels. PNVF nanogels were purified by centrifugation at 15 000 rpm for 45 min followed by removal of supernatant. The nanogel pellets were dispersed in water pH ~8 (~20 mL) and then dialyzed against water pH ~8 controlled by using sodium carbonate (molecular weight cutoff = 2000 Da for blank nanogels and 100 000 Da for nanogels containing lysozyme).

Characterization of Materials and Nanogels. A Bruker AMX 500 spectrometer was used to record the NMR spectra of the BDEP cross-linker synthesized using deuterated chloroform ($CDCl_3$) as a solvent and tetramethylsilane as an internal standard. Particle sizes and size distributions of nanogels were determined by dynamic light scattering (Brookhaven Zeta-PALS). The mean effective diameter and polydispersity were determined according to the method of cumulants.[28] The dissolution kinetics of acid-labile PNVF nanogels were determined as a function of pH using Brookhaven BI-MAS software. The dissolution kinetics of nanogels were further confirmed at various pHs by measuring the optical density of samples over time using an 8453 UV/vis spectrophotometer (Agilent Technologies) following methods previously reported.[25,26] Briefly, ~9−10 mg of nanogels was placed into a cuvette containing 3 mL of buffer solution at a given pH. The optical density was measured at a fixed wavelength of 480 nm at 25 °C at preselected intervals until the solution became clear. TEM images of nanogels were obtained using A JEOL 1200 EXII transmission electron microscope operating at an accelerating voltage of 80 kV. AFM images of nanogels were obtained using an Optizoom atomic force microscope and Digital Instruments Nanoscope 3A.

Nanogel and PNVF Toxicity Study. Cell viability was assessed using a CellTiter 96 AQueous Cell Proliferation assay kit (Promega). Briefly, human umbilical cord vascular endothelial cells (HUVEC) were seeded in 96-well tissue culture plates at a density of 8000 cells/well and cultured in DMEM medium supplemented with 10% heat inactivated bovine serum. Cells were then incubated with 100 μL of polymer samples diluted at various concentrations in the cell culture medium for another 24 h. Then, 20 μL of MTS ([3-(4,5-dimethylthiazol-2-yl)-5-(3-carboxymethoxyphenyl)-2-(4-sulfophenyl)-2*H*-tetrazolium]) and PMS (phenazine methosulfate) were added and incubated for 4 h before reading the absorbance at 490 nm with a 96-well plate reader (Molecular Devices Corp.). Cell viability was expressed as the percentage of absorbance relative to the control (cells not exposed to the material). Experiments were performed in triplicate, with eight replicate wells for each sample and control per assay.

Lysozyme Release Study for Acid-Labile PNVF Nanogels. Lysozyme-loaded PNVF nanogels (40 mg) were dispersed either in 8 mL of sodium phosphate buffer, pH 7.4, or acetic acid buffer (pH 5.8) at 37 °C. The suspension was divided into four aliquots and put in centrifuge tubes. At reported time intervals, the nanogels were collected by centrifugation and the supernatant was sampled. The samples were loaded in 96-well plate by placing 120 μL of sample/well. When FITC-lysozyme was used, fluorescence was determined using a Microplate reader (SpectraMax M5, Molecular Devices Corp., San Francisco, CA) set to 490 nm excitation and 525 nm emission. When lysozyme was used, the protein concentration was determined by using a bicinchoninic acid (BCA) assay (Pierce). All samples were performed in triplicate. The percent release was defined as the ratio of the concentration of protein in the hydrolyzed supernatant compared to that found in the completely hydrolyzed supernatant solutions (i.e., measured protein mass/protein loading mass).

Enzymatic Activity Assay of Lysozyme. The enzymatic activity of lysozyme was determined by using an assay based on the hydrolysis of the outer cell membrane of *Micrococcus lysodeikticus* (Sigma-Aldrich Inc.). Samples of stock or released lysozyme were diluted to a concentration of about 50 μg/mL. A total of 10 μL of sample was added to 250 μL of *M. lysodeikticus* suspension (0.3 mg/mL bacteria in 100 mM phosphate buffer, pH 6.2), and the decrease in turbidity was measured for 5 min at 450 nm using a Microplate reader (SpectraMax M5, Molecular Devices Corp.). Experiments were conducted in triplicate and normalized to the protein concentration as determined by using the BCA assay. Results were determined according to the initial kinetic rate (slope of optical density vs time) as recommended by the supplier. A calibration curve of stock lysozyme was made over the appropriate concentration range (10−120 μg/mL).

Table 1. Properties of PNVF Nanogels for Different Reaction Conditions

run	NVF (mg)	BDEP (mg)	diameter (nm) in hexane (polydispersity)	diameter (nm) in water (polydispersity)	yield (%)
1[a]	350	50	86.1 (0.061)	127.9 (0.011)	98.1
2[b]	350	50	73.8 (0.045)	122.3 (0.067)	89.3

[a] Polymerization temperature: 50 °C. Polymerization time: 24 h. [b] Polymerization temperature: 35 °C. Polymerization time: 48 h.

Gel Permeation Chromatography and SDS−PAGE Analysis of Recovered Lysozyme. Blank nanogels and nanogels containing lysozyme were hydrolyzed by incubating with 50 mM acetate buffer (pH 5.0) for 5 h at 37 °C. The recovered protein was purified by using a cation exchange cartridge (Sep-PakAccell plus CM, 6CC 500 mg base, Waters Corp.) and eluted with 10 mM phosphate buffer pH from 4.7 to 3.1 and 0−500 mM NaCl. The extract was dialyzed against water using dialysis membrane tubing MWCO 10 kDa (Spectrapor, Spectrum Laboratories Inc.) and concentrated by using 5 kDa centrifugal filter (Amicon, Millipore Corp.).

The protein extract samples were examined by using sodium dodecyl sulfate−polyacrylamide gel electrophoresis (SDS−PAGE) and gel permeation chromatography (GPC). SDS−PAGE was performed on vertical slab gel (NuPAGE4−12% Bis-Tris Gel, Invitrogen). Protein extract samples or standard lysozyme were mixed with sample buffer and heated at 70 °C for 10 min, and then 10−35 μL of standards or samples were applied to the gel. Electrophoresis was conducted at 120 mA for 30 min, and samples were visualized by staining with Coomassie Brilliant Blue R-250. For GPC studies, the protein extract samples and standard lysozyme were injected in a gel permeation apparatus (LC-10AT pump, SIL-10AXL autoinjector, SPD-10A UV−vis detector, and LC-Class VP workstation software, Shimadzu Co., Kyoto, Japan) equipped with a GPC column (ShodexSB-803HQ, 8 mm i.d. × 30 cm, JM Science Inc.). The mobile phase was 50 mM phosphate buffer pH 7.0 containing 300 mM NaCl, and a flow rate of 0.3 mL/min was used. Finally, the aggregation of recovered lysozyme was examined by using a dynamic light scattering system (BT 9000AT) equipped with a 50 mW HeNe laser with a 532 nm emission wavelength (Brookhaven Instruments Corp., Holtsville, NY). Scattered light was monitored at 90 °C to the incident beam.

Results

PNVF Nanogel Production Depended on Reaction Conditions. The hydrophilicity of NVF monomers and of the resulting PNVF made this polymer an attractive candidate for encapsulating proteins into nanogels; however, methods needed to be developed to determine reaction conditions that provided the desired particle size and acceptable process yields at low temperature. Typically, higher temperatures, often >50 °C, are utilized to speed free radical polymerization and production of cross-linked gel particles.[29] A low temperature free radical initiator was tested (VAZO-52) to make the process more amenable to protein encapsulation. The effect of temperature on the process was monitored. Polymerization reactions at the lower temperature required 48 h to generate yields of ~90% in comparison to the high yield (~98%) achieved at 50 °C in half the time (Table 1).

Dynamic light scatting was also employed to analyze nanogel size and size distribution throughout the polymerization reaction. The hydrodynamic sizes of nanogels were measured in the polymerized microemulsion and in deionized water (Table 1).

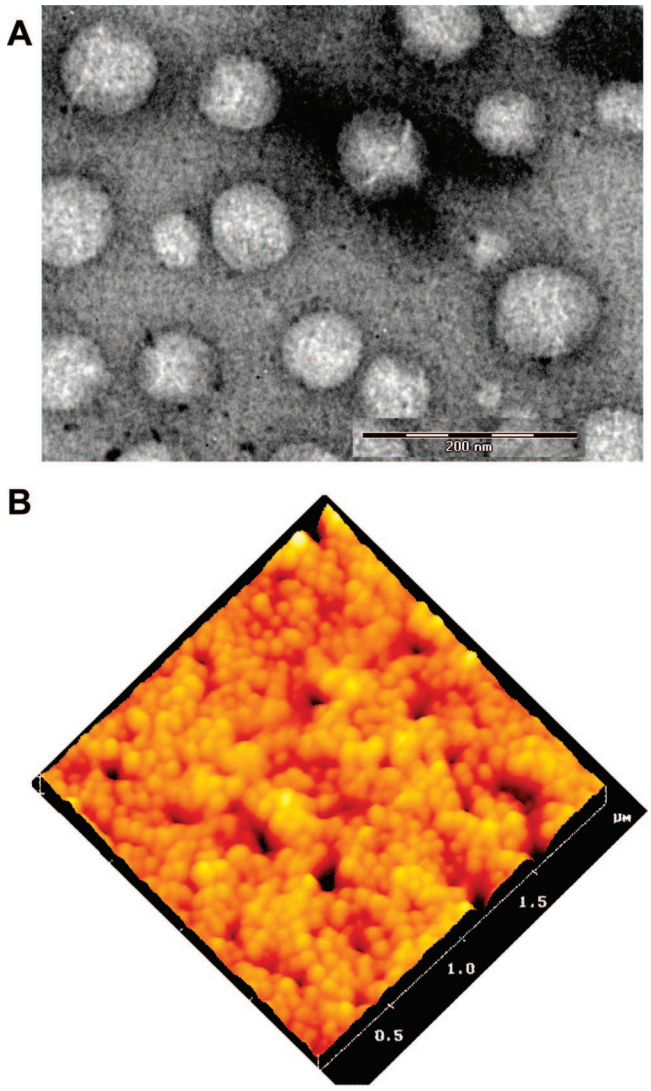

Figure 2. (A) Transmission electron micrographs and (B) atomic force micrographs showed that nanogels possessed a smooth, rounded morphology.

The final particle size was similar for polymerization reactions occurring at 50 °C (24 h) and at 35 °C (48 h); however, particle size increased much more slowly at 35 °C than at 50 °C (Figure 1B). These data suggested that the size of nanogels could be regulated by both polymerization temperature and time, albeit at the cost of decreasing yield. Nanogel sizes were also observed to be smaller in hexane than in water, suggesting that the nanogel swelled as a result of additional hydrogen bonding with water upon transfer out of the hexane continuous phase (Table 1). Dynamic light scattering studies further confirmed that PNVF nanogels had relatively low polydispersity.

Microscopic techniques were used to probe nanogel morphology. Using transmission electron microscopy (TEM), nanogels were observed to be spherical with a somewhat ruffled surface (Figure 2A). The observed morphology was expected since nanogels must be imaged in a dry state when using TEM. Atomic force microscopy (AFM) was also employed as a means to determine the structure of hydrated nanogels. Dry nanogels were soaked in water, transferred onto a glass plate, and imaged using AFM. Images of acid-labile PNVF nanogels (14.3% cross-linker) demonstrated a smooth, spherical morphology (Figure 2B). Image analysis software determined nanogel size to be roughly 100 nm, which provided further credence to dynamic light scattering data.

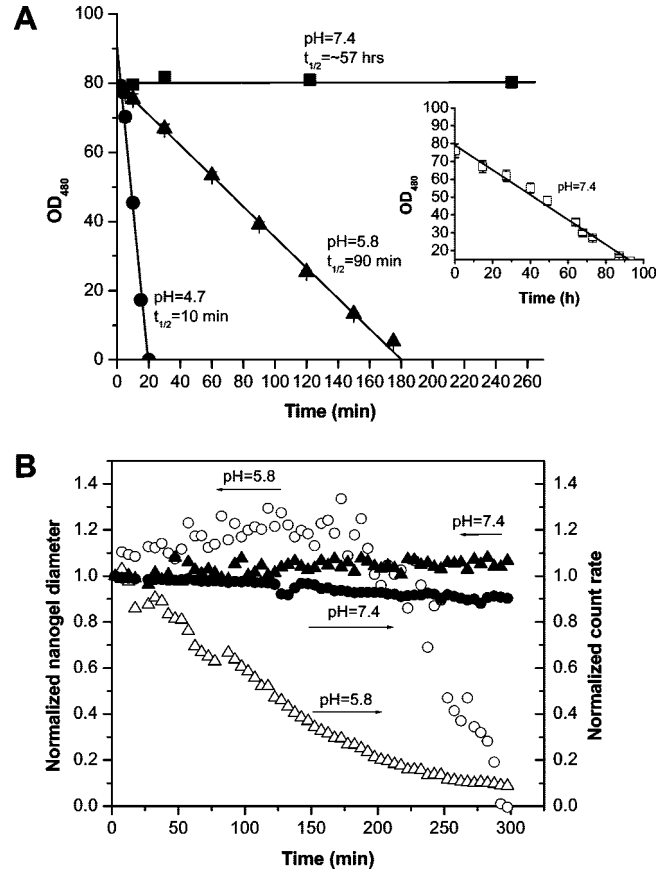

Figure 3. (A) Degradation of PNVF nanogels over time strongly depended upon media pH as determined by a turbidity assay (optical density) of an acid-labile PNVF nanogel suspension over time. Linear trendlines were fit to the data as a method to estimate the nanogel dissolution half-life. Nanogel cross-linking density used for these experiments was 5.3%. (B) Degradation kinetics of acid-labile PNVF nanogels (~200 nm) over time was confirmed using dynamic light scattering. Data were normalized to facilitate direct comparison. At pH 7.4, the nanogel size remained constant, and the count rate deceased slightly. At pH 5.8, the count rate decreased more rapidly, and the size remained constant prior to a rapid decrease.

PNVF Nanogels Cross-Linked with BDEP Degraded Rapidly at Low pH. The degradation kinetics of PNVF nanogels was strongly dependent on the pH of the surrounding milieu because the hydrolysis rate of ketals under acidic conditions is proportional to the hydronium ion concentration in solution as previously discussed in work by Frechet and others.[30] The degradation kinetics of acid-labile PNVF nanogels was initially quantified using a turbidity assay, which allowed direct observation of the transition of nanogel colloids from opaque suspensions to tranparent solutions. Nanogel suspensions containing 3 mg/mL were chosen so that the initial optical density was close to 100% (Figure 3A). The decrease in the optical density of the suspension was monitored at 480 nm over time. The reduction in optical density indicated the corresponding degradation kinetics of PNVF nanogels. Upon complete degradation of nanogels, the sample was nearly clear. PNVF nanogels cross-linked with the ketal-containing cross-linker degraded much more rapidly at acidic pH than at physiological pH. The relative half-life of PNVF nanogels (5.3% cross-linker) was estimated from the midpoint of a linear fit to the optical density data (Figure 3A). Acid-labile PNVF nanogels showed increased stability at neutral pH (pH 7.4; $t_{1/2} > 56$ h) compared to rapid dissolution observed at lower pH (pH 4.7; $t_{1/2} \sim 10$ min).

The degradation kinetics and change in particle size of PNVF nanogels were also quantified by dynamic light scattering. Using this method, the particle size and average count rate can be

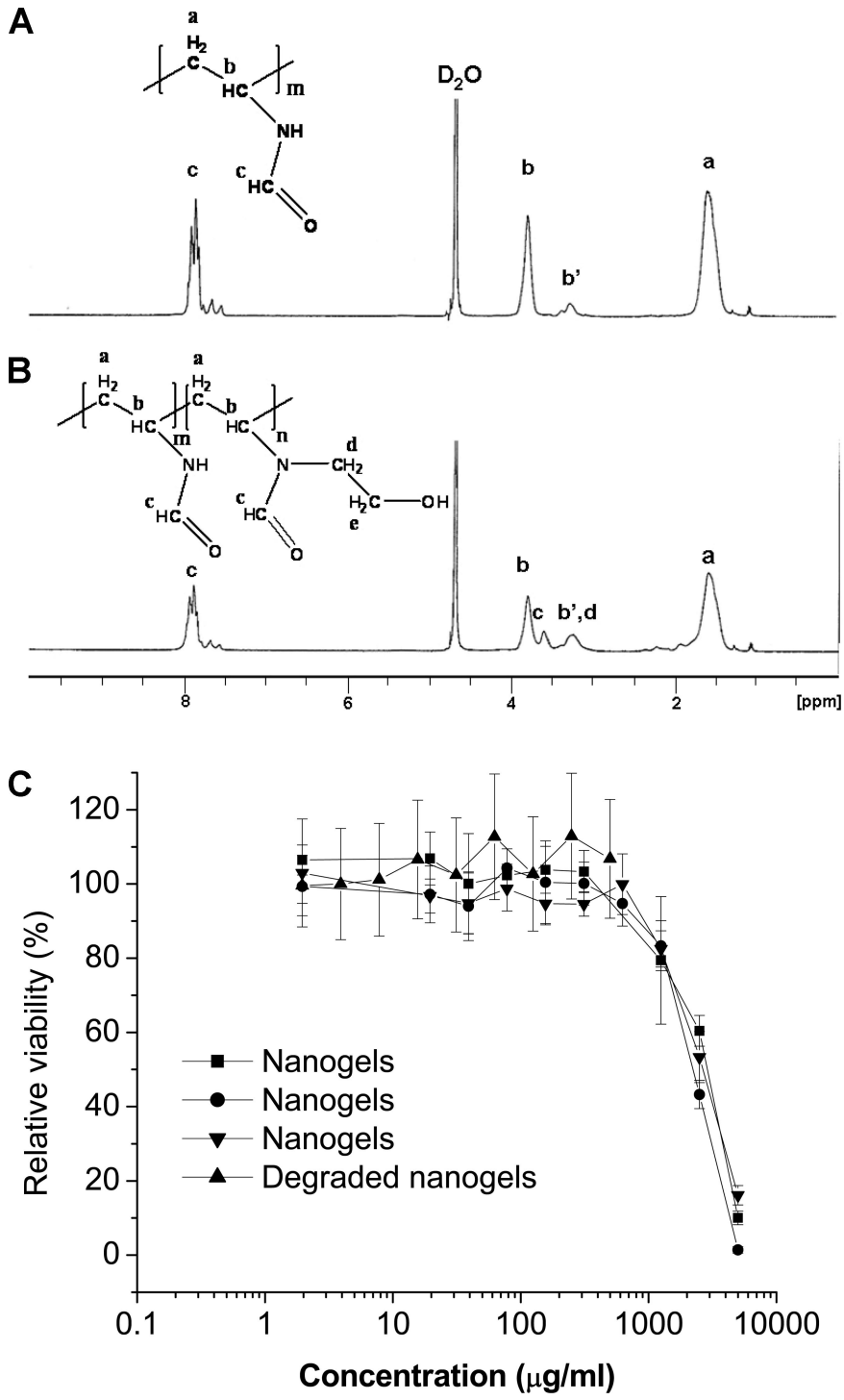

Figure 4. (A) ^{1}H NMR spectra of PNVF and (B) PNVF with BDEP residue obtained by degradation of PNVF in 10% HF. (C) Cytotoxicity of nanogels ($n = 3$) and degraded nanogels (PNVF oligomer) against HUVEC was determined to be >1 mg/mL.

determined over time as a function of pH (Figure 3B). Average count rate is a measurement of light scattering events with units of kilocounts per second (kCPS), which varies directly with the product of particle size and concentration. The diameter and count rate were normalized to facilitate direct comparison of nanogel changes at different pH values. The size of acid-labile PNVF nanogels did not change markedly at pH 7.4; however, the count rate came down gradually, suggesting that nanogel dissolution was occurring slowly. Conversely, the nanogel size at pH 5.8 was observed to increase slightly and then decrease rapidly. The average count rate decreased quickly over time at pH 5.8, confirming that nanogels dissolved much faster at pH 5.8 than at pH 7.4. Taken cumulatively, these results also suggest that nanogels degrade in the bulk of the particle, which caused a slight particle swelling as the cross-linker degraded, followed by complete and rapid dissolution of the nanogels.

Nanogels and Nanogel Degradation Products Exhibited Minimal Cytotoxicity. The chemical structure of the polymer remaining after nanogel degradation was determined by ^{1}H NMR. The existence of BDEP residue on PNVF oligomers after ketal linkage breakdown was confirmed (Figure 4). Compared to the proton NMR spectrum of PNVF, a new proton peak at 3.60 ppm was ascribed to the protons ($-CH_2CH_2OH$) of the BDEP residue. The molecular weight of PNVF oligomers remaining after degradation of PNVF nanogels was measured

Table 2. FITC-Lysozyme and Lysozyme Encapsulation Performance in PNVF Nanogels[a]

monomer (mg)	cross-linker (mg)	yield (%)	hydrodynamic diameter (nm) (polydispersity)	zeta potential (mV)	protein encapsulation efficiency (%) BCA	protein encapsulation efficiency (%) fluorescence	lysozyme activity after release (%)
388	12.5	50.74	190.7 (0.264)	−4.32 ± 1.15	37.06 ± 3.86	37.17 ± 2.51	49.14 ± 1.47
375	25	62.17	202.6 (0.311)	−5.29 ± 1.71	46.80 ± 2.70	45.70 ± 0.27	45.21 ± 0.50
350	50	60.21	180.6 (0.312)	−5.10 ± 1.05	41.93 ± 1.06	45.81 ± 5.30	51.54 ± 2.33
388	12.5	51.80	178.5 (0.287)	−3.08 ± 1.10	45.08 ± 1.91		39.01 ± 1.56
375	25	61.26	183.1 (0.307)	−4.09 ± 1.86	63.82 ± 4.35		64.57 ± 1.66
350	50	58.00	162.9 (0.307)	−4.71 ± 3.03	65.30 ± 0.75		61.65 ± 0.12
350	50	66.94	92.9 (0.307)	−7.08 ± 0.80			

[a] Polymerization condition; 37 °C for 24 h. Top set = FITC-lysozyme; middle set = lysozyme; bottom row = control (no lysozyme).

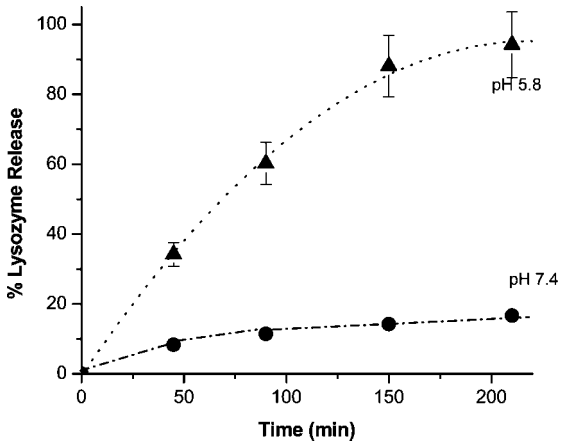

Figure 5. Release profiles of lysozyme from acid labile PNVF nanogels (cross-linker 10%).

by size exclusion chromatography. The molecular weight of the recovered nanogel residue was ~14.8 kDa. The viability of human umbilical cord vascular endothelial cells (HUVEC) was assessed as a function of the concentration of nanogels and degraded nanogels (Figure 4C). A cytotoxicity study showed that both the nanogels and the polymer resulting from degraded nanogels had an IC_{50} value >1 mg/mL.

Nanogels Released Active Lysozyme with Kinetics Determined by pH. Lysozyme was encapsulated in PNVF nanogels in order to study the release kinetics from acid-labile PNVF nanogels as a function of pH. Inverse emulsion polymerization reactions were carried out in the same fashion as before, except that 10 mg of lysozyme was included in the aqueous phase with the 400 mg of monomer and cross-linker. The theoretical loading achieved using this process would, therefore, be 2.5% (w/w). The size and zeta potential of lysozyme-loaded PNVF nanogels polymerized using various ratios of monomer to cross-linker did not change significantly (Table 2). The size of nanogels nearly doubles, however, compared to the same polymerization reaction without lysozyme (bottom row). Interestingly, the encapsulation efficiency of lysozyme decreased significantly when FITC was used as a fluorescent tag on lysozyme. Only approximately one FITC molecule was conjugated to each lysozyme molecule; however, the hydrophobic nature of this dye may have adversely affected lysozyme encapsulation. The reduced encapsulation efficiency of FITC-lysozyme was corroborated by fluorescence and BCA quantification methods.

A release study was carried out at 37 °C under the common physiological condition of pH 7.4 and under an acidic environment (pH 5.8) to simulate a pH that may be encountered intracellularly after endocytosis. The drug release from PNVF nanogels at pH 7.4 was very slow. Only about 15% of encapsulated lysozyme was released after 200 min (Figure 5). Conversely, drug release from PNVF nanogels at pH 5.8 was significantly faster with about 95% of encapsulated protein releasing within the same time window. These experimental results demonstrated that acid labile PNVF nanogels differentially release their payload under acidic conditions.

The activity of lysozyme was also tested after release was completed. For these studies, a suspension of the outer cell membrane of *Micrococcus lysodeikticus* was incubated with lysozyme released from PNVF nanogels. The change in the turbidity of this cell membrane suspension was tracked over time and was compared to a calibration curve employing stock lysozyme. FITC-labeled lysozyme released from nanogels retained about half of the original activity of the FITC-labeled lysozyme stock (Table 2; top set). In addition, lysozyme was only encapsulated with about 40% efficiency in PNVF nanogels using the lowest cross-linker content, but encapsulation efficiency increased significantly with higher cross-linker content. Formulations using a higher amount of cross-linker also demonstrated a significantly greater lysozyme activity which approached a maximum of ~65% (Table 2; middle set).

The loss of lysozyme activity was largely attributed to protein aggregation. Gel permeation chromatography was conducted on stock lysozyme and yielded a single peak with a retention time around 52 min. Lysozyme released from PNVF nanogels showed a similar peak; however, a large second peak also appeared around 20 min (Figure 6A). The shorter retention time of the new peak indicated that the lysozyme had significantly aggregated. SDS-PAGE studies were conducted to determine whether the lysozyme aggregates were irreversible when treated with this strong detergent (SDS) and heating (70 °C for 10 min). Only a single band was noted for the lysozyme that was released from PNVF nanogels, and the mobility corresponded to that of lysozyme used in the size standard (Figure 6B), indicating that lysozyme aggregates could be disrupted. Finally, analysis of lysozyme recovered from nanogels was conducted using dynamic light scattering. Lysozyme aggregates ranged from 8 to 40 nm in diameter compared to a diameter of ~2 nm detected for lysozyme stock solutions.

Discussion

The hydrophilic nature of gel materials makes them desirable for the controlled delivery of proteins and other biological agents. Some of the first gel materials were larger matrices where the encapsulation and release of active ingredients was dominated by diffusion through the mesh polymer network. The polymer mesh size is determined by multiple factors including the molecular weight of the polymer and the degree of cross-links, either physical or chemical. PNVF nanoparticles reported here demonstrated relatively efficient lysozyme encapsulation when the monomer to cross-linker ratio was at least 15 (Table 2). Insignificant improvement in the encapsulation efficiency of lysozyme was observed at lower monomer to cross-linker ratios, suggesting that a critical mesh size was attained at a monomer to cross-linker ratio of 15.

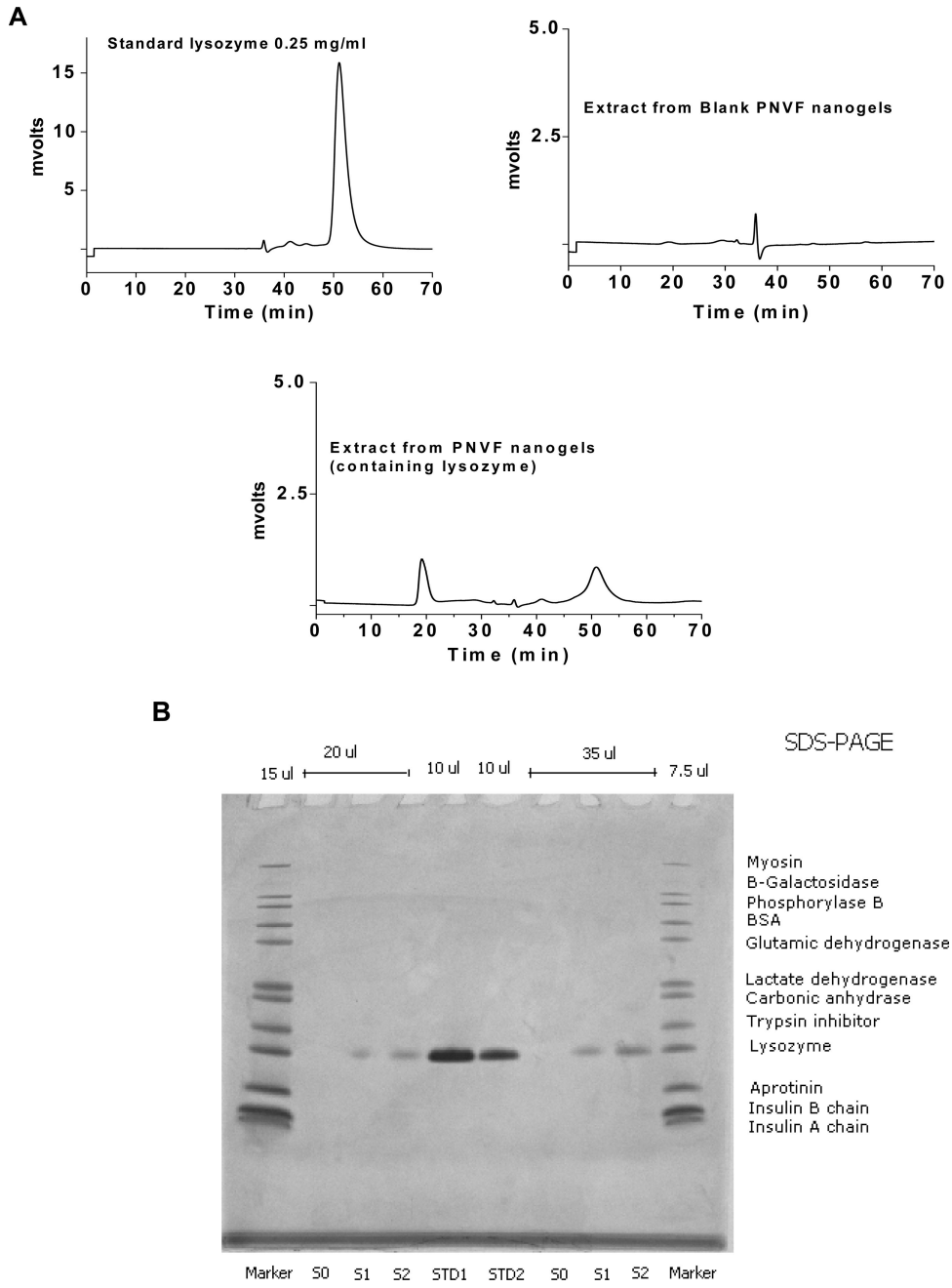

Figure 6. (A) Gel permeation chromatograms showed a shorter retention time for lysozyme recovered from nanogels suggesting that lysozyme aggregates existed. (B) SDS−PAGE analysis of lysozyme indicated that the molecular weight of the recovered protein was unchanged. S0 = extract from blank PNVF NGs; S1 = extract from PNVF NGs containing lysozyme; S2 = extract from PNVF NGs containing lysozyme; STD1 = standard lysozyme 2 μg; STD2 = standard lysozyme 1 μg.

Researchers have developed two primary approaches for modulating the release rate of active ingredients from gel materials in an effort to broaden applications. First, the retention and release rate of proteins may be modulated by utilizing polymers that interact with the active ingredient. For example, the release of growth factors complexed with heparin may be slowed by modifying gels to include peptides that bind to the complex and decrease the effective diffusion coefficient of the complex.[31] Alternatively, the inclusion of a labile bond within the polymer backbone or within the cross-linker has yielded gel materials that can achieve much more precise control of the delivery of active ingredients. For example, Frechet and others developed acid-labile gel microspheres 200−500 nm in diameter as vehicles to deliver vaccines.[32] Acid-labile microspheres were reported to be able to release their payload into the cytoplasm of dendritic cells as a result of the low pH encountered in lysosomes. This finding is especially critical when trying to deliver protein therapeutics that may be subject to deactivation or degradation as a result of the lower pH and proteolytic enzymes present in lysosomes.

Inverse microemulsions may represent a preferred method for forming micro- and nanoparticles from hydrogel materials. Similar methods to the one reported here have been used to encapsulate proteins with retention of native structure.[16] Tween-80 and Span-80 were employed as cosurfactants to get an optimal hydrophile lipophile balance, and both are FDA approved. A stable optically transparent inverse microemulsion was obtained by emulsifying pH 8.0 PBS solution containing an appropriate amount of monomers and initiator (VAZO-52) into hexane phase containing Tween-80 and Span-80 surfactants. The solution transitioned to translucent or opaque as the polymerization reaction proceeded. Using these conditions, it

was found that polymerization should be carried out at 35 °C or above; otherwise, no particles will be formed.

Although lysozyme retained more than half of its activity, work remains to improve nanogel processing conditions so that more fragile protein therapeutics may be delivered via these materials. As an aid to recommend potential improvements to the reported polymerization strategy, a few activity assays were conducted on lysozyme at each stage of release from PNVF nanogels. This study showed that lysozyme released at very early time points (hours) did not exhibit substantial activity (typically <5−10%). It is hypothesized that lysozyme released early may have been present at the hydrophobic hexane/surfactant interface during polymerization. Future work in this area should aim to minimize protein exposure to this source of denaturation. Some excellent work has already been conducted on two-phase aqueous systems as a potential improvement to inverse microemulsion polymerization approaches.[33]

The ultimate goal for nanoparticle delivery systems is to improve localization of therapeutic agents (e.g., subcellularly, intratumorally, etc.) to enhance therapeutic efficacy and mitigate systemic toxicity or side effects. Attaining this goal will require continued efforts to improve the compatibility of nanoparticles with biological fluids and to enhance nanoparticle recognition of delivery sites. The hydrophilicity of nanogels makes them desirable for intravenous administration since agglomeration, opsonization, and clearance may be reduced in comparison to hydrophobic or charged particles. In addition, researchers seek to modify nanoparticle surfaces to attain tissue specificity and aim to adjust material properties to allow selective drug release. High sensitivity to pH was observed with the cross-linker synthesized for these studies, BDEP. Besides intracellular drug delivery, this type of differential release of proteins has also been hypothesized to be beneficial for the delivery of chemotherapeutic agents due to the slight acidity often associated with tumor tissue. Continued progress may lead to nanoparticles that effectively localize drugs as a means to improve efficacy and mitigate side effects.

Conclusions

Synthesis of hydrogel nanoparticles provides the opportunity to extend the applications of gel materials. In this report, *N*-vinylformamide (NVF) was polymerized in the aqueous phase of an inverse emulsion and was cross-linked using an acid-labile cross-linker, 2-bis[2,2′-di(*N*-vinylformamido)ethoxy]propane. Methods were developed to polymerize NVF at low temperature (35 °C) to enable the encapsulation of protein therapeutics, which are often sensitive to thermal denaturation at higher temperatures. Lysozyme was used as a model protein, and after 200 min, 95% of the lysozyme was released at pH 5.8 compared to only 15% release at pH 7.4. A minimum of 3% cross-linker was necessary to achieve a reasonable encapsulation efficiency of ∼40%, and increasing the cross-linker concentration allowed >60% of the lysozyme to be encapsulated. Typically, at least half of the activity of lysozyme was retained. Acid-sensitive PNVF nanogels were also minimally cytotoxic to vascular endothelial cells, suggesting that these nanoparticles may be suitable for intravenous administration. Future studies aim to elucidate the pharmacokinetics of nanogels to determine whether the hydrophilicity of these materials will enable long circulation half-life in comparison to other nanomaterials.

Acknowledgment. We are grateful for funding from the American Heart Association, the NIH (R03 AR054035, P20 RR016443, and P20 RR015563), and the Cystic Fibrosis Foundation for supporting portions of this research. We also thank Prof. C. Russ Middaugh and Prof. Robert Dunn for the use of laboratory equipment and The Microscopy Laboratory for assistance with TEM imaging.

References and Notes

(1) Lowman, A. M.; Peppas, N. A. In Mathiowitz, E., Ed.; *Encyclopedia of Controlled Drug Delivery*; John Wiley and Sons: New York, 1999; Vol. *1*, pp 397−418.
(2) van de Wetering, P.; Metters, A. T.; Schoenmakers, R. G.; Hubbell, J. A. Poly(ethylene glycol) hydrogels formed by conjugate addition with controllable swelling degradation and release of pharmaceutically active proteins. *J. Controlled Release* **2005**, *102* (3), 619–627.
(3) Silva, E. A.; Mooney, D. J. Spatiotemporal control of vascular endothelial growth factor delivery from injectable hydrogels enhances angiogenesis. *J. Thromb. Haemostasis* **2007**, *5* (3), 590–598.
(4) Serra, L.; Domenech, J.; Peppas, N. A. Drug transport mechanisms and release kinetics from molecularly designed poly(acrylic acid-g-ethylene glycol) hydrogels. *Biomaterials* **2006**, *27* (31), 5440–5451.
(5) Hori, K.; Sotozono, C.; Hamuro, J.; Yamasaki, K.; Kimura, Y.; Ozeki, M.; Tabata, Y.; Kinoshita, S. Controlled-release of epidermal growth factor from cationized gelatin hydrogel enhances corneal epithelial wound healing. *J. Controlled Release* **2007**, *118* (2), 169–176.
(6) Cai, S.; Liu, Y.; Zheng Shu, X.; Prestwich, G. D. Injectable glycosaminoglycan hydrogels for controlled release of human basic fibroblast growth factor. *Biomaterials* **2005**, *26* (30), 6054–6067.
(7) Hwang, S. J.; Park, H.; Park, K. Gastric retentive drug-delivery systems. *Crit. Rev. Ther. Drug Carrier Syst.* **1998**, *15* (3), 243–284.
(8) Wang, J.; Chua, K. M.; Wang, C. H. Stabilization and encapsulation of human immunoglobulin G into biodegradable microspheres. *J. Colloid Interface Sci.* **2004**, *271* (1), 92–101.
(9) Cadee, J. A.; de Groot, C. J.; Jiskoot, W.; den Otter, W.; Hennink, W. E. Release of recombinant human interleukin-2 from dextran-based hydrogels. *J. Controlled Release* **2002**, *78* (1−3), 1–13.
(10) Elisseeff, J.; McIntosh, W.; Fu, K.; Blunk, B. T.; Langer, R. Controlled-release of IGF-I and TGF-beta1 in a photopolymerizing hydrogel for cartilage tissue engineering. *J. Orthop. Res.* **2001**, *19* (6), 1098–1104.
(11) Van Tomme, S. R.; De Geest, B. G.; Braeckmans, K.; De Smedt, S. C.; Siepmann, F.; Siepmann, J.; van Nostrum, C. F.; Hennink, W. E. Mobility of model proteins in hydrogels composed of oppositely charged dextran microspheres studied by protein release and fluorescence recovery after photobleaching. *J. Controlled Release* **2005**, *110* (1), 67–78.
(12) Nie, T. Baldwin, A. Yamaguchi, N. Kiick, K. L., Production of heparin-functionalized hydrogels for the development of responsive and controlled growth factor delivery systems. *J. Controlled Release*, in press.
(13) Sutter, M.; Siepmann, J.; Hennink, W. E.; Jiskoot, W. Recombinant gelatin hydrogels for the sustained release of proteins. *J. Controlled Release* **2007**, *119* (3), 301–312.
(14) Megeed, Z.; Haider, M.; Li, D.; O'Malley, B. W., Jr.; Cappello, J.; Ghandehari, H. In vitro and in vivo evaluation of recombinant silk-elastinlike hydrogels for cancer gene therapy. *J. Controlled Release* **2004**, *94* (2−3), 433–445.
(15) Hart, D. S.; Gehrke, S. H. Thermally associating polypeptides designed for drug delivery produced by genetically engineered cells. *J. Pharm. Sci.* **2007**, *96* (3), 484–516.
(16) Delgado, M.; Spanka, C.; Kerwin, L. D.; Wentworth, P., Jr.; Janda, K. D. A tunable hydrogel for encapsulation and controlled release of bioactive proteins. *Biomacromolecules* **2002**, *3* (2), 262–271.
(17) Leach, J. B.; Schmidt, C. E. Characterization of protein release from photocrosslinkable hyaluronic acid-polyethylene glycol hydrogel tissue engineering scaffolds. *Biomaterials* **2005**, *26* (2), 125–135.
(18) Hennink, W. E.; De Jong, S. J.; Bos, G. W.; Veldhuis, T. F.; van Nostrum, C. F. Biodegradable dextran hydrogels crosslinked by stereocomplex formation for the controlled release of pharmaceutical proteins. *Int. J. Pharm.* **2004**, *277* (1−2), 99–104.
(19) de Jong, S. J.; van Eerdenbrugh, B.; van Nostrum, C. F.; Kettenes-van, J. J.; Hennink, W. E. Physically crosslinked dextran hydrogels by stereocomplex formation of lactic acid oligomers: degradation and protein release behavior. *J. Controlled Release* **2001**, *71* (3), 261–275.
(20) Vinogradov, S. V. Colloidal microgels in drug delivery applications. *Curr. Pharm. Des.* **2006**, *12* (36), 4703–4712.
(21) Bulmus, V.; Chan, Y.; Nguyen, Q.; Tran, H. L. Synthesis and characterization of degradable p(HEMA) microgels: use of acid-labile crosslinkers. *Macromol. Biosci.* **2007**, *7* (4), 446–455.
(22) Murthy, N.; Xu, M.; Schuck, S.; Kunisawa, J.; Shastri, N.; Frechet, J. M. A macromolecular delivery vehicle for protein-based vaccines: acid-degradable protein-loaded microgels. *Proc. Natl. Acad. Sci. U.S.A.* **2003**, *100* (9), 4995–5000.
(23) Panyam, J.; Labhasetwar, V. Biodegradable nanoparticles for drug and gene delivery to cells and tissue. *Adv. Drug Delivery Rev.* **2003**, *55* (3), 329–347.

(24) McAuley, K. B. The chemistry and physics of polyacrylamide gel dosimeters: why they do and don't work. *J. Phys. Conf. Ser.* **2004**, *3*, 29–33.
(25) Shi, L.; Berkland, C. pH-Triggered Dispersion of Nanoparticle Clusters. *Adv. Mater.* **2006**, *18* (17), 2315–2319.
(26) Shi, L.; Berkland, C. Acid-Labile Polyvinylamine Micro- and Nanogel Capsules. *Macromolecules* **2007**, *40* (13), 4635–4643.
(27) Berkland, C.; Pollauf, E.; Raman, C.; Silverman, R.; Kim, K.; Pack, D. W. Macromolecule release from monodisperse PLG microspheres: control of release rates and investigation of release mechanism. *J. Pharm. Sci.* **2007**, *96* (5), 1176–1191.
(28) Koppel, D. E. Analysis of macromolecular polydispersity in intensity correlation spectroscopy: the method of cumulants. *J. Chem. Phys.* **1972**, *57* (11), 4814–4820.
(29) Gu, L.; Zhu, S.; Hrymak, A. N.; Pelton, R. H. Kinetics and modeling of free radical polymerization of N-vinylformamide. *Polymer* **2001**, *42*, 3077–3086.
(30) Goh, S. L.; Murthy, N.; Xu, M.; Frechet, J. M. Cross-linked microparticles as carriers for the delivery of plasmid DNA for vaccine development. *Bioconjugate Chem.* **2004**, *15* (3), 467–474.
(31) Sakiyama-Elbert, S. E.; Hubbell, J. A. Controlled release of nerve growth factor from a heparin-containing fibrin-based cell ingrowth matrix. *J. Controlled Release* **2000**, *69* (1), 149–158.
(32) Kwon, Y. J.; James, E.; Shastri, N.; Frechet, J. M. In vivo targeting of dendritic cells for activation of cellular immunity using vaccine carriers based on pH-responsive microparticles. *Proc. Natl. Acad. Sci. U.S.A.* **2005**, *102* (51), 18264–18268.
(33) Jain, S.; Yap, W. T.; Irvine, D. J. Synthesis of protein-loaded hydrogel particles in an aqueous two-phase system for coincident antigen and CpG oligonucleotide delivery to antigen-presenting cells. *Biomacromolecules* **2005**, *6* (5), 2590–2600.

MA800812Z